Isotropic and nondispersive planar fed Luneburg lens from Hamiltonian transformation optics

Oscar Quevedo-Teruel, Wenxuan Tang, and Yang Hao*

School of Electronic Engineering and Computer Science, Queen Mary University of London Mile End Road, London, UK

**Corresponding author: yang.hao@eecs.qmul.ac.uk*

Received August 31, 2012; revised October 16, 2012; accepted October 16, 2012; posted October 17, 2012 (Doc. ID 175416); published November 22, 2012

A modified Luneburg lens based on Hamiltonian optical transformation with planar feeds is proposed in this Letter. The lens, made of conventional all-dielectric materials, does not have any kind of anisotropy. Therefore, in theory, its bandwidth of operation has no upper frequency limitations in contrast with recent designs utilizing metamaterials. Results for wide-angle radiation and broadband operation are presented.

OCIS codes: 080.3620, 080.3630, 220.3620, 220.3630.

Luneburg lenses, proposed in 1944 [1], have the ability of focusing the fields in the opposite direction of arrival of electromagnetic fields. In particular, they can transform spherical waves into plane-waves at a certain distance, which is defined by the size of the lens. Moreover, any external electromagnetic field arriving from outside of the lens is gradually matched (avoiding any reflection) to the feed and vice versa. This is a very important advantage of this kind of lens with respect to other gradient index lenses discussed in the literature, such as Tarhanov's or Ilinsky's lenses [2,3].

However, in spite of their impressive properties, Luneburg lenses have not been often employed for practical applications because their shape (a dielectric sphere composed of concentric dielectric variations) has to be fed at its curved edges in order to obtain wide-angle radiations, which presents practical difficulties of implementation and manufacturing [4].

A possible solution to this problem, by using transformation optics, has been recently proposed [5], and a demonstrator was designed and measured after applying some simplifications, which avoided the use of permittivities lower than unity. Therefore, since the structure is not necessarily resonant (i.e., it is less dispersive), it presents a decent band of operation. However, the use of transformation optics may introduce anisotropic properties and the particular implementation in [5,6], based on equivalent refraction indexes produced by periodic repetitions of metallic inclusions, limits the band of operation of the device.

In this Letter, we demonstrate how Hamiltonian optics (corpuscular theory of light) can be employed to modify the shape of Luneburg lenses [4], in order to obtain equivalent results of those proposed in [5], but avoiding any kind of anisotropy and also significantly improving its operating bandwidth and directivity.

Luneburg lenses were initially defined by dielectric materials in a spherical shape presenting a variable refraction index [1]. Particularly, these lenses can be implemented as a dielectric sphere in which its permittivity changes with the space position according to the following expression [3,7]:

$$\epsilon_r = 2 - \left(\frac{r}{R}\right)^2 \qquad (1)$$

where r is the position in spherical coordinates from the center of the lens and R is the radius, which defines the size of the lens. This expression is graphically represented in Fig. 1(a) for a two-dimensional (2D) configuration when $R = 3\lambda$. As it can be seen, the permittivity of the lens changes from $\epsilon_r = 1$ in the external part of the sphere to $\epsilon_r = 2$ in the inner part. Therefore, any external incoming wave will be gradually matched to the lens, and there will be no reflections. In Fig. 1(b), we illustrate the field distribution after applying a normal line source to the lens in Fig. 1(a). As predicted, a cylindrical wave is transformed into a plane-wave in the opposite side of the lens. This calculation was carried out by using a 2D in-house FDTD simulator as described in [8,9].

Conventionally, the focus of a Luneburg lens can be shifted to inside the lens by using Hamiltonian optics (corpuscular theory of light), being the dielectric constant distribution in the following [4]:

$$\epsilon_r = \frac{1 + \left(\frac{f}{R}\right)^2 - \left(\frac{r}{R}\right)^2}{\left(\frac{f}{R}\right)^2}, \qquad (2)$$

where f is the distance from the center to the focus. The dielectric constant distribution for this modified

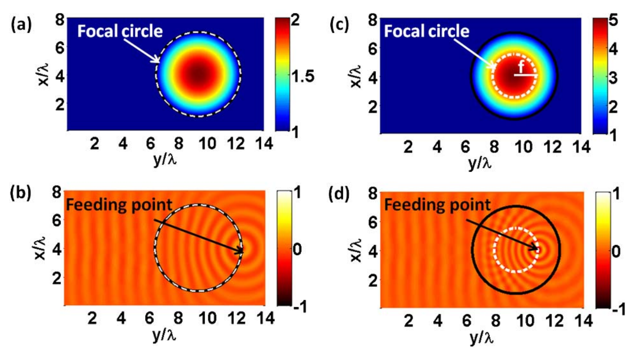

Fig. 1. (Color online) (a),(b) Conventional Luneburg lens: (a) 2D permittivity map of a Luneburg lens following the expression of Eq. (1) when $R = 3\lambda$; (b) normalized field distribution in the Luneburg lens when it is fed from one of its edges with a normal line source. (c),(d) Modified Luneburg lens: (c) 2D permittivity map of a Luneburg lens following the expression of Eq. (2) when $R = 3\lambda$ and $f = R/2$; (d) normalized field distribution in the modified Luneburg lens when it is fed with a normal line source in its focal point.

0146-9592/12/234850-03$15.00/0

Luneburg lens is represented in Fig. 1(c) when $R = 3\lambda$ and $f = R/2$. As Fig. 1(d) illustrates, when a normal line source is placed at any point on the focal circle (denoted as a white-dashed circle), located at a distance f from the center, a plane-wave is produced at the opposite side of the lens (its edge is outlined as a black solid circle).

After this, the transformation of the Luneburg lens in which the focal point is shifted inside the lens so that the focal circle radius is decreased and therefore the distance between potential focal points is smaller; thus, the curved feeding plane can accurately be approximated by a flat plane as illustrated in Fig. 2(a). In order to demonstrate a feasible practical implementation, a dielectric discretization of eight layers has been also carried out. The dimension R has been selected to be 3.33λ, which is a similar size along the y axis as the lens presented in [5], and f has been chosen to be $0.25R$ in order to have a maximum dielectric constant comparable to the one proposed also in [5].

In order to evaluate the proposed design, a parallel-plate waveguide configuration has been considered [5], enabling the excitation and transmission of an E_z polarization. To make the results more realistic, losses have been included in all the materials ($\tan\delta = 0.01$). The simulated results with commercial software (CST Microwave Studio) for different feeding positions in the x axis are illustrated in Fig. 2. The lens presents excellent properties until approximately 60°, although the maximum angle of beam steering can be even wider with a slight increase in sidelobe levels and degradation in the main radiation beam.

The main advantage of this design, with respect to others in which equivalent refractive indexes are employed [5], is the absence of dependance on the frequency (at higher values). In Fig. 3 results for different frequencies (5, 15, and 25 GHz) at two angles of radiation (0° and 60°) are presented. We can certainly assert that the performance of the lens is not affected by the

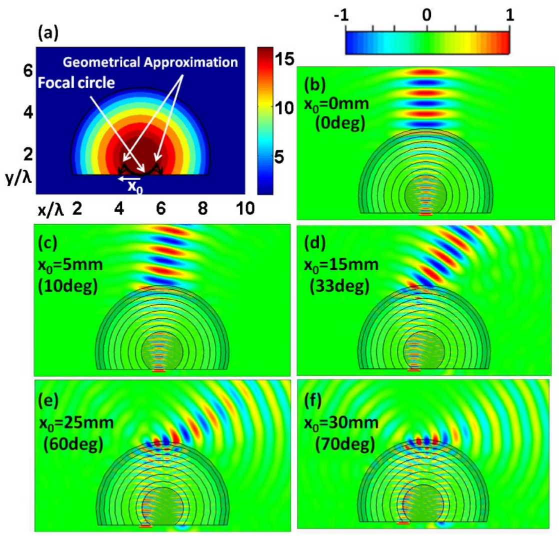

Fig. 2. (Color online) (a) 2D permittivity map of a modified Luneburg lens with a planar shape of feeding after eight layers discretization, with $R = 3.33\lambda$ and $f = 0.25R$. (b)–(f) E_z component at 10 GHz for different positions of the feeding ($x_0 = 0$ mm to $x_0 = 30$ mm).

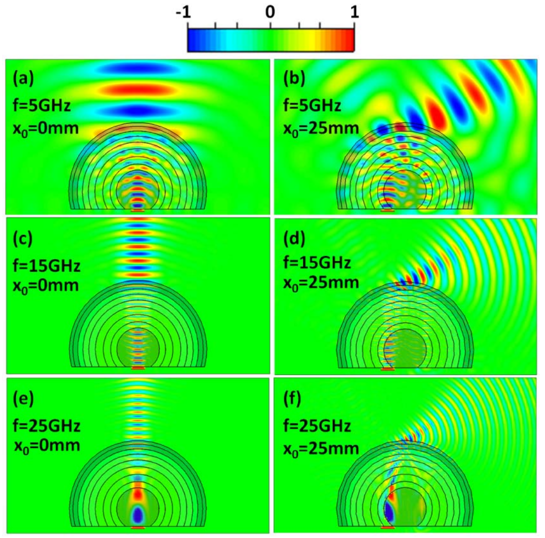

Fig. 3. (Color online) E_z component at different frequencies for two positions of the feeding ($x_0 = 0$ mm and $x_0 = 25$ mm).

increase of the frequency. In contrast, the bandwidth of the metamaterial-designs proposed in the literature is always limited [10,11], although a wider band of operation may be achieved by using dielectric constants higher than unity [5,6]. For example, in the metallic dogbone-shaped configuration proposed in [5,6], when the frequency is increased, the different equivalent materials start to operate inadequately, thereby degrading the performance of the device. In order to provide a comparison of this previous work with respect to the modified Luneburg lens proposed in this Letter, the normalized electric far field of both lenses at 10 and 21 GHz are shown in Figs. 4(a), 4(b). Although both lenses work adequately at the original frequency of operation (10 GHz); at 21 GHz the lens proposed in [5] works improperly due to its intrinsic dispersive properties; while the modified Luneburg lens proposed in this Letter maintains its properties. Moreover, the E-field distribution obtained by a 2D in-house dispersion FDTD code is shown in Fig. 4(c) for comparison. This field is calculated at more than 6λ from the center, although still in the near-field region. The results agree with the 3D simulations carried out with the commercial software at 10 GHz (Fig. 4(a)). In Fig. 4(c), it is demonstrated how the use of materials with $\epsilon_r \leq 1$ in the lens proposed in [5] does not affect the results in the broadside direction, although when the angle becomes more extreme, the performance is degraded. This indicates that broad-angle radiation can be achieved by using metamaterials (ignoring anisotropy) but only with a narrow-bandwidth. However, a true broad-angle lens can only be achieved by the use of active metamaterials [12–14]. In addition, the simulations with both software corroborate that the beam at the broadside direction is more directive in the proposed modified Luneburg lens, presenting a clear advantage for antenna applications. In order to give an estimation of the results, the simulated directivity for the case of the proposed design is 10.5 dB at 10 GHz and 13.6 dB at 21 GHz for the broadside direction, while for the case of the lens proposed in [5], it is 6.4 dB at 10 GHz and 7.53 at 21 GHz. For the case of 60° of inclination, in the proposed design it is

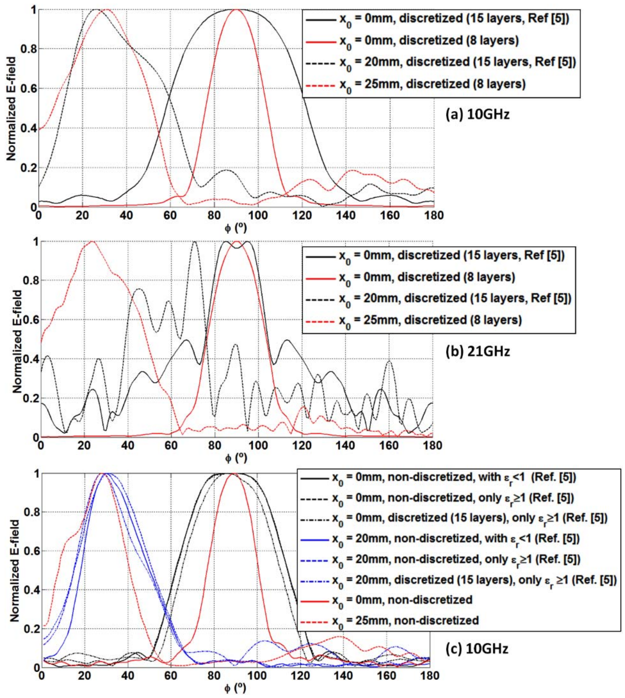

Fig. 4. (Color online) (a),(b) CST Microwave Studio simulation of normalized electric far field at two different frequencies (10 and 21 GHz) for two positions of the feeding in the proposed modified Luneburg lens and the one presented in [5]. The discretization is 15 layers for the lens presented in [5] and only eight layers for the proposed modified Luneburg lens. (c) Electric field distribution for a 2D in-house FDTD simulation at 10 GHz for the proposed modified Luneburg lens and the one presented in [5] for two positions of the feeding. Different simulations are presented: continuous variation of the dielectric map, including or not materials with $\epsilon_r \leq 1$, and discretized maps (15 layers for the case of [5]).

7.6 dB at 10 GHz and 11.4 dB at 21 GHz, while in the lens proposed in [5] it is 7.7 dB at 10 GHz and 8.2 dB at 21 GHz. As a final result, we illustrate in Fig. 4(c) how the discretization affects the performance of the device proposed in [5] (increasing the scattering in some undesired directions), thus demonstrating the increased robustness of the modified lens proposed in this Letter over those of practical dielectric constant discretizations.

A completely isotropic and nondispersive Luneburg lens with planar feed locations has been proposed and studied in this Letter. This work demonstrates that despite what recent scientific contributions have demonstrated [5,6], the use of metamaterials, and particularly dispersive and anisotropic materials has to be more carefully reviewed and compared with classical theories and design techniques.

The proposed lens has been demonstrated to work from 5–30 GHz, although, in theory, there are no limitations at higher frequencies of operation except the ones derived from permittivity variations due to the quality of the employed materials. The lens provides a beam steering from 0° to 60° with a good performance, and it can be applied to any polarization thus making it suitable for any 3D beam steering application.

The authors are grateful to the Office of Naval Research Global (ONRG) under Naval International Cooperative Opportunities (NICOP) for the funding support with Grant No. N00014-09-1-1013.

References

1. R. Luneburg, *Mathematical Theory of Optics* (Brown University, 1944).
2. R. Ilinsky, J. Opt. A **2**, 449 (2000).
3. A. Demetriadou and Y. Hao, Opt. Express **19**, 19925 (2011).
4. A. S. Gutman, J. Appl. Phys. **25**, 855 (1954).
5. N. Kundtz and D. R. Smith, Nat. Mater. **9**, 129 (2010).
6. R. Liu, C. Ji, J. J. Mock, J. Y. Chin, T. J. Cui, and D. R. Smith, Science **323**, 366 (2009).
7. A. Demetriadou and Y. Hao, IEEE Antennas Wireless Propag. Lett. **10**, 1590 (2011).
8. Y. Zhao, C. Argyropoulos, and Y. Hao, Opt. Express **16**, 6717 (2008).
9. Y. Hao and R. Mittra, *FDTD Modeling of Metamaterials: Theory and Applications* (Artech House, 2008).
10. B. Nistad and J. Skaar, Phys. Rev. E **78**, 036603 (2008).
11. K. Palmer, IEEE Spectrum **49**, 13 (2012).
12. S. Tretyakov and S. Maslovski, IEEE Antennas Propag. Mag. **49**, 37 (2007).
13. K. Z. Rajab, Y. Hao, D. Bao, C. G. Parini, J. Vazquez, and M. Philippakis, J. Appl. Phys. **108**, 054904 (2010).
14. S. Hrabar, I. Krois, I. Bonic, and A. Kiricenko, Appl. Phys. Lett. **99**, 254103 (2011).